Electronic Structure and the Properties of Metals. II. Application to Zinc

WALTER A. HARRISON
General Electric Research Laboratory, Schenectady, New York
(Received 22 October 1962)

The method developed in the preceding paper for computing properties of metals from first principles is applied to zinc. The OPW form factors which determine many electronic properties and the characteristic function of wave number which determines many atomic properties are computed and applied to sample properties. Those properties treated are the Fermi surface, electronic specific heat and cyclotron resonance, the resistivity due to vacancies, the resistivity of the liquid, the electron-phonon interaction, the crystal structure and c/a ratio, the energy change on melting, the structure and energy of formation of vacancies, the elastic constants, the "stabilization" of ordered structures in alloys, phonon structure and dispersion, and the Kohn effect. Where comparison of calculated electronic properties with experiment was possible the agreement was good. Agreement with experiment was more limited for the atomic properties, though the discrepancies appeared to be consistent with the uncertainty in the interpolations used in obtaining the energy-wave-number characteristic. Such a discrepancy was finding the fcc structure lower in energy than the hcp structure; this also gave rise to instability against the formation of certain phonons. Otherwise the agreement for the atomic properties was semiquantitative. It is suggested that irregularities found by Brockhouse, Rao, and Woods in the phonon spectrum of lead are not images of the Fermi surface, but images of the energy-wave-number characteristic. Such fluctuations depend upon the detailed structure of the atom and are found to be much larger than those associated with the Kohn effect; in zinc they occur at wave numbers near, but not exactly at, $2k_F$. The appearance of these irregularities suggests the possibility of computing the energy-wave-number characteristic, and therefore a wide range of properties, from such measurements of the phonon spectrum along symmetry directions.

The possibility of obtaining the essential results of the theory with simpler approximations is considered, as well as the possibility of improving on the method.

I. INTRODUCTION

In the preceding communication[1] (which we will call I) a method was formulated for the calculation from first principles of a variety of electronic and atomic properties of metals. This formulation entailed three approximations: (1) the self-consistent field approximation, (2) the assumption that the core states are the same as in the free atom, and (3) a perturbation solution, carried to second order, of the Hamiltonian matrix based upon orthogonalized plane waves. We now proceed to apply this method to a specific metal in order to see what features of the approach are important in physical problems and to provide an experimental check on the validity of the method.

We select zinc for the reasons outlined in our earlier analysis[2] of the band structure and Fermi surface of zinc (which we will call O). This calculation is, in fact, a direct extension of O.

The computations beyond those carried out in the treatment O were performed by hand. This entailed more interpolation of computed results and grosser numerical approximations than one would wish. Consequently, they do not provide as accurate an experimental check as would be possible with a machine calculation.

We will first outline the computation which was performed, noting in particular the numerical approximations which were involved. We present the computed OPW form factors which determine the interesting matrix elements of the pseudopotential, the energy-wave-number characteristic which determines the dependence of the band-structure energy, on the reciprocal lattice, and the equivalent effective ion-ion interaction. We then proceed to computations of a number of interesting properties and compare these with experiment where possible.

II. COMPUTATION OF MATRIX ELEMENTS

We found in I that it was possible to write the total energy and the scattering rates in terms of matrix elements between plane waves of a pseudopotential, W. Further, it was found that these matrix elements could be separated into two factors,

$$\langle \mathbf{k}+\mathbf{q}|W(k)|\mathbf{k}\rangle = S(\mathbf{q})\langle \mathbf{k}+\mathbf{q}|w(k)|\mathbf{k}\rangle. \quad (2.1)$$

The structure factor, $S(\mathbf{q})$, is given by

$$S(\mathbf{q}) = (1/N)\textstyle\sum_j \exp(-i\mathbf{q}\cdot\mathbf{r}_j), \quad (2.2)$$

the sum being over the ion positions $\mathbf{r}_j$; this factor depends only upon the ion positions, not upon the ion potential. The remaining factor, which we called the OPW form factor, depends only upon the ionic potential and the average ion density. This OPW form factor is to be computed self-consistently, but the first step requires the determination of matrix elements of an l-dependent ionic potential, v_{op}', which does not contain the field due to the conduction electrons and which is cut off at a sphere of volume equal to the atomic cell volume. The remainder of the potential, v, which includes the self-consistent field of the conduction electrons as well as the tails of the Coulomb field of the ion beyond the equivalent sphere, is then included separately.

[1] W. A. Harrison, preceding paper [Phys. Rev. **129**, 2503 (1963)].
[2] W. A. Harrison, Phys. Rev. **126**, 497 (1962).

1. Matrix Elements from the Truncated Ion Potential

The matrix elements of the pseudopotential based on the potential v_{op}' were written in I [see Eq. (4.8)] as

$$\langle \mathbf{k}+\mathbf{q}|w(k)|\mathbf{k}\rangle-\langle \mathbf{k}+\mathbf{q}|v|\mathbf{k}\rangle = \langle \mathbf{k}+\mathbf{q}|u|\mathbf{k}\rangle+\frac{\langle \mathbf{k}|u|\mathbf{k}\rangle}{1-\sum_t \langle \mathbf{k}|t\rangle\langle t|\mathbf{k}\rangle} \times\sum_t \langle \mathbf{k}+\mathbf{q}|t\rangle\langle t|\mathbf{k}\rangle, \quad (2.3)$$

with [see Eq. (4.7)]

$$\langle \mathbf{k}+\mathbf{q}|u|\mathbf{k}\rangle=\langle \mathbf{k}+\mathbf{q}|v_{op}'|\mathbf{k}\rangle -\sum_t \langle t|v_{op}'|\mathbf{k}\rangle\langle \mathbf{k}+\mathbf{q}|t\rangle. \quad (2.4)$$

Here the matrix elements are written in terms of the potential, v_{op}', and the normalized core wave functions, ψ_t, centered on an ion at $r=0$. Writing the cell volume Ω_0, these become

$$\langle \mathbf{k}+\mathbf{q}|v_{op}'|\mathbf{k}\rangle=\Omega_0^{-1}\int e^{-i(\mathbf{k}+\mathbf{q})\cdot\mathbf{r}}v_{op}'e^{i\mathbf{k}\cdot\mathbf{r}}d\tau,$$

$$\langle t|v_{op}'|\mathbf{k}\rangle=\Omega_0^{-1/2}\int \psi_t^* v_{op}'e^{i\mathbf{k}\cdot\mathbf{r}}d\tau, \quad (2.5)$$

$$\langle \mathbf{k}+\mathbf{q}|t\rangle=\Omega_0^{-1/2}\int e^{-i(\mathbf{k}+\mathbf{q})\cdot\mathbf{r}}\psi_t d\tau.$$

In O we computed such integrals with k and $|\mathbf{k}+\mathbf{q}|$ always equal to the Fermi wave number. The "unscreened" potential used there was the same as v_{op}' except for a muffin-tin cutoff rather than a cutoff at the equivalent sphere. v_{op}' is an l-dependent potential; hence, it was necessary to expand the exponentials in spherical harmonics and spherical Bessel functions in the integrations. Only a small number of such integrations were necessary; the matrix elements for general relative orientation of $\mathbf{k}$ and $\mathbf{k}+\mathbf{q}$ were then given as an analytic function of the angle between them. In I we found that this was also true if $|\mathbf{k}+\mathbf{q}|$ were given some fixed value different from k. The analytic form may be written

$$\langle \mathbf{k}+\mathbf{q}|w|\mathbf{k}\rangle-\langle \mathbf{k}+\mathbf{q}|v|\mathbf{k}\rangle =A(q)+\sum_l B_l(|\mathbf{k}+\mathbf{q}|,k)P_l(\cos 2\Theta). \quad (2.6)$$

The $P_l(\cos 2\Theta)$ are Legendre polynomials of

$$\cos 2\Theta=(\mathbf{k}+\mathbf{q})\cdot\mathbf{k}/|\mathbf{k}+\mathbf{q}|k;$$

i.e., 2Θ is the angle between $\mathbf{k}$ and $\mathbf{k}+\mathbf{q}$. The term

$$A(q)=-\frac{4\pi Ze^2}{\Omega_0}\int_0^{r_s}\frac{\sin qr}{qr}rdr$$

derives from the net ion potential, $-Ze^2/r$, within the equivalent sphere of radius r_s. The remainder of v_{op}' is included in the B_l. We include only the terms to $l=2$. For larger l values there would be a contribution from the self-consistent field, but none from exchange. The values of the B_l which we have computed are given in Table I.

TABLE I. $B_l(k',k_F)$ in Ry.

	$k'/k_F=0$	1	2	3	4
$l=0$	0.3417	0.3123	0.1881	0.0991	0.0470
$l=1$	0	0.0580	0.0810	0.0691	0.0433
$l=2$	0	0.0256	0.0192	0.0189	0.0036

The calculation gave also "OPW overlaps" in the form

$$\sum_t \langle \mathbf{k}+\mathbf{q}|t\rangle\langle t|\mathbf{k}\rangle=\sum_l C_l(|\mathbf{k}+\mathbf{q}|,k)P_l(\cos 2\Theta). \quad (2.7)$$

The computed values of the C_l are given in Table II.

The values in Table I, when interpolated for intermediate values of k', may be inserted into Eq. (2.6) to give matrix elements for a sizable range of final states but only for initial states on the Fermi surface. For computing the self-consistent field and for computing the total energy we will need matrix elements for all initial states within the Fermi surface. A set of these might be calculated as were the values with initial states on the Fermi surface. We might, on the other hand, construct an interpolation formula for the matrix elements computed above and use this formula for all initial and final states. We have followed the latter procedure. Such a formula makes possible the analytic integration over occupied states and permits a hand calculation. The formula could be improved by fitting to a larger number of points computed as above.

We first make the interpolation of the OPW overlaps,

$$\sum_t \langle \mathbf{k}+\mathbf{q}|t\rangle\langle t|\mathbf{k}\rangle=\sum_n b_n(q)[\mathbf{k}\cdot(\mathbf{k}+\mathbf{q})]^n, \quad (2.8)$$

and then write the interpolation of the OPW form factors,

$$\langle \mathbf{k}+\mathbf{q}|w(k)|\mathbf{k}\rangle =\sum_n [a_n(q)+(\hbar^2k^2/2m)b_n(q)][\mathbf{k}\cdot(\mathbf{k}+\mathbf{q})]^n. \quad (2.9)$$

This is not a general form; but it has a number of desirable features. (1) It was found possible to fit a number of computed matrix elements, for fixed q, with only three terms in the expansion. (2) It behaves properly under the interchange of initial and final states. This behavior required the inclusion of the b_n term in Eq. (2.9) to give the nonhermiticity of the matrix

TABLE II. $C_l(k',k_F)$.

	$k'/k_F=0$	1	2	3	4
$l=0$	0.0863	0.0745	0.0488	0.0255	0.0098
$l=1$	0	0.0298	0.0378	0.0310	0.0207
$l=2$	0	0.0338	0.0460	0.0396	0.0260

elements calculated in I [Eq. (3.9)]. (3) It provides a continuation into the region where no calculations have been made. (4) It allows a term-by-term analytic integration when we sum over occupied states.

In our computation we interpolated Tables I and II to give the B_l and C_l for $k'/k_F=0.5$, 1.5 and 2.5. For each value of q this gave us up to five matrix elements and OPW overlaps, corresponding to different values of k' and different relative orientations of $\mathbf{k}$ and $\mathbf{k}'$. These were fit with three terms in Eqs. (2.8) and (2.9) for q/k_F in half-integral steps from 0 through 3.0. This gave us, for fixed $\mathbf{q}$, an analytic form for the matrix elements as a function of $\mathbf{k}$.

2. Matrix Elements from the Unscreened Potential

The pseudopotential matrix elements described above are based upon the truncated ion potential v_{op}'. We add to these the matrix elements associated with the tails of the truncated ion potential and those associated with the charge density due to orthogonalization. Both of these are simple potentials and give, therefore, functions of q only.

The number of (positive) electronic charges localized by the orthogonalization in the region of each nucleus is readily seen to be the average over $k<k_F$ of $Z\sum_l \langle\mathbf{k}|l\rangle\langle l|\mathbf{k}\rangle=Zb_0(0)=Z\sum_l C_l(k,k)$. From Table II we obtain the value $0.138Z=0.276$. We approximate this localized charge by a point charge; thus the addition of the tails of the Coulomb potential and the charge due to orthogonalization gives the matrix elements of the unscreened potential in the form of the right-hand side of Eq. (2.6) with $A(q)$ replaced by $1.138Z4\pi e^2/q^2\Omega_0$ and the B_l remain the same as in Table I.

3. Matrix Elements from the Screened Potential

In I we found the screening potential, in terms of the matrix elements of the uncreened pseudopotential, w^0, to be given by[3]

$$v_q^{sc}=\frac{\dfrac{4\pi e^2}{q^2\Omega}\sum_{k<k_F}\left\{\dfrac{\langle\mathbf{k}+\mathbf{q}|w(k)^0|\mathbf{k}\rangle}{T_k-T_{k+q}}+\dfrac{\langle\mathbf{k}-\mathbf{q}|w(k)^0|\mathbf{k}\rangle^*}{T_k-T_{k-q}}\right\}}{1-\dfrac{4\pi e^2}{q^2\Omega}\sum_{k<k_F}\left\{\dfrac{1}{T_k-T_{k+q}}+\dfrac{1}{T_k-T_{k-q}}\right\}}. \tag{2.10}$$

We note that if the matrix elements were independent of $\mathbf{k}$ they could be taken outside of the summation in the numerator and the result written in terms of the Hartree dielectric function: $v_q^{sc}=\langle\mathbf{k}+\mathbf{q}|w(k)^0|\mathbf{k}\rangle(1-\epsilon_q)/\epsilon_q$. This, however, is not the case and we must substitute the analytic form for the uncreened matrix elements in the summation. The summation is converted to an integral and performed term by term for each value of q (again taking q in half-integral steps from 0 to 3). The angular integration was performed first; then the integral from $k=0$ to k_F.

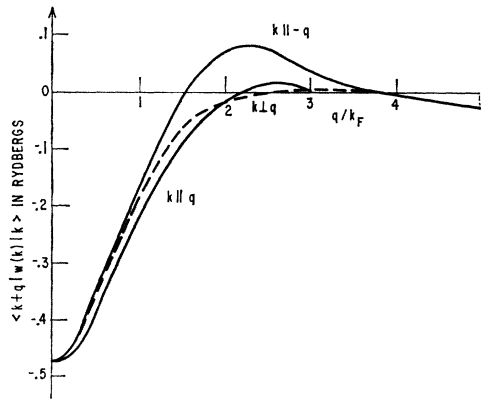

FIG. 1. The OPW form factors for zinc at the observed density and for k equaling the Fermi wave number, k_F. The three curves for different orientations of $\mathbf{k}$ and $\mathbf{q}$ would be the same if the pseudopotential could be written as a simple potential. Matrix elements of the pseudopotential are obtained by multiplying these form factors by a structure factor depending only on the positions of the ions.

This v_q^{sc} is added to the unscreened form factors to obtain the final self-consistent OPW form factors. The matrix elements which enter all of our calculations are proportional to these form factors.

We have plotted a series of computed form factors as a function of q for three relative orientations of $\mathbf{k}$ and $\mathbf{q}$ in Fig. 1. The curves are drawn through computed points at the half-integral values of q/k_F. Values above $q=3k_F$ are obtained by noting that the screening field is negligible in this region, and carrying Eq. (2.6) as far as possible with the B_l values given in Table I.

Several features of the curves are worth noting. The $q=0$ limit is given by

$$\lim_{q\to 0}\langle\mathbf{k}+\mathbf{q}|w(k)|\mathbf{k}\rangle=-[\tfrac{2}{3}+0.1381(1-k^2/k_F^2)]E_F.$$

The curves plotted are for $k=k_F$, so the limiting form factor is simply the free-electron value $-\frac{2}{3}E_F$. Thus we would obtain the usual limit to the interaction between electrons and long wavelength longitudinal phonons, but would obtain corrections to the Bohm-Staver[4] calculation of the speed of sound.

We note the rapid decrease in the magnitude of the form factors near $q=2k_F$ as the repulsive terms in the

[3] As in I, the summation over $\mathbf{k}$ implies a summation also over spin.

[4] D. Bohm and T. Staver, Phys. Rev. 84, 836 (1950).

pseudopotential become important. This is responsible for the nearly-free-electron-like character of the Fermi surface.

We note the spread between the three curves, especially near $q=2k_F$, indicating the importance of the l-dependent potential and the corresponding breakdown of any wave-number-independent pseudopotential approximation.

We note the apparently rapid decrease in the form factors at large q which is necessary if the OPW method is to converge rapidly.

The particular set of OPW form factors connecting two states which both lie on the Fermi surface is of particular interest and is plotted in Fig. 2. This is the set which enters first-order scattering and which determines the Fermi surface. Again values were computed only at half-integral q/k_F. The experimental values listed are from fitting the experimental surface in the paper O.

III. EVALUATION OF THE ENERGY

In I we divided the total energy of the crystal into three terms: (1) the free-electron energy, which is independent of the arrangement of the ions and therefore need not be evaluated for the problems we discuss; (2) the electrostatic energy, which is equal to the Coulomb energy of a set of point positive charges at the ion positions and with charge equal to $Z^*=Z(1-0.138^2)^{1/2}=1.981$ for zinc imbedded in a compensating uniform negative background; and (3) the band structure energy given by

$$E_{bs}=\sum_q S^*(\mathbf{q})S(\mathbf{q})E(q), \tag{3.1}$$

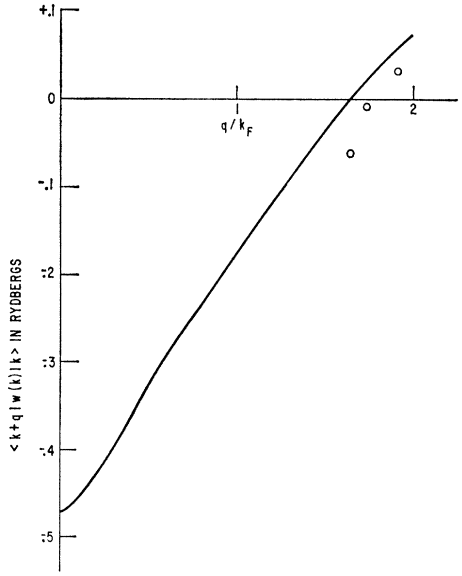

FIG. 2. The OPW form factors for zinc at the observed density and for k and $|\mathbf{k}+\mathbf{q}|$ equaling the Fermi wave number, k_F. These form factors determine all matrix elements which enter first-order scattering and are predominant in determining the Fermi surface. The three experimental points are from the "experimental band structure" of zinc determined earlier (see reference 2).

TABLE III. $E(q)$ in Ry per electron.

q/k_F	$E(q)$
0	$-\infty$
0.5	−1.08
1	−0.0368
1.5	+0.00198
1.75	+0.00158
2.0	−0.00048
2.25	−0.00322
2.5	−0.000697
3	−0.000238

per electron with $E(q)$, the energy-wave-number characteristic, given by

$$E(q)=\frac{1}{NZ}\sum_{k<k_F}\Big[-\langle\mathbf{k}+\mathbf{q}|w(k)^0|\mathbf{k}\rangle\sum_t\langle\mathbf{k}|t\rangle\langle t|\mathbf{k}+\mathbf{q}\rangle + \frac{|\langle\mathbf{k}+\mathbf{q}|w(k)|\mathbf{k}\rangle|^2}{T_k-T_{k+q}}-\frac{\Omega_0 q^2}{4\pi Ze^2}|v_q^{sc}|^2 + v_q^{sc}\sum_t\Big(\langle\mathbf{k}-\mathbf{q}|t\rangle\langle t|\mathbf{k}\rangle - \langle\mathbf{k}|t\rangle\langle t|\mathbf{k}\rangle\int\psi_t^*\psi_t e^{i\mathbf{q}\cdot\mathbf{r}}d\tau\Big)\Big]. \tag{3.2}$$

In the final sum over core states we again treat the ions as small, and set $\int\psi_t^*\psi_t e^{i\mathbf{q}\cdot\mathbf{r}}d\tau=1$. We may then readily show that the contribution of the final sum over t to $E(q)$ is $v_q^{sc}b_2(q)q^2k_F^2/5$ which turns out to be negligible compared to the other contributions to $E(q)$, as suggested in I, and it is dropped.

The other contributions may be computed directly from the parameters computed above. The sum over $k<k_F$ is converted to an integral as in the computation of the screening field, but the evaluation is much more laborious. For the term in which the form factor appears squared we end up with well over one hundred terms by the time all integrations are performed. This gives us values of $E(q)$ for half-integral values of q/k_F through 3.0. We also obtained values for $q/k_F=1.75$ and 2.25 by interpolating the $a_n(q)$ and $b_n(q)$. The values obtained are listed in Table III and are plotted in Fig. 3.

We will use this $E(q)$ function directly in all of the computations of band-structure energy to be made here. As indicated in I, we may transform this curve and add the Coulomb interaction to obtain an effective two-body interaction between ions. We wrote $x=q/k_F$, and found the effective interaction $\mathcal{U}(r)$ given by

$$\mathcal{U}(r)=\frac{3Z^2}{k_F r}\int_0^\infty x\sin k_F r x E(k_F x)dx+Z^{*2}e^2/r. \tag{3.3}$$

This calculated interaction is tabulated in Table IV and plotted in Fig. 4. The rather striking minimum occurs at approximately the nearest-neighbor distance in zinc.

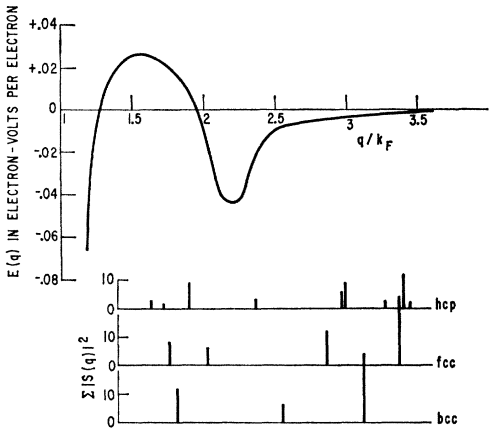

FIG. 3. The energy-wave-number characteristic for zinc at the observed density. The band-structure energy is obtained by summing the product of the characteristic and the square of the magnitude of the structure factor over reciprocal lattice vectors, $E_{bs}=\Sigma_{\mathbf{q}}|S(\mathbf{q})|^2E(q)$. $|S(\mathbf{q})|^2$ times the number of reciprocal lattice vectors with magnitude equal to $q/2\pi$ is plotted below for hcp (at the observed c/a), fcc, and bcc structures.

The oscillatory character arises from the general shape of the $E(q)$ curve rather than from singularities in $E(q)$ at $q=2k_F$. We might also note that the Born-Mayer potential is monotonic rather than oscillatory as we find.

The use of $\mathcal{V}(r)$ avoids the necessity of separate electrostatic energy computations. For all of the problems we treat we find it more convenient to use the formulation with $E(q)$ and to compute the change in electrostatic energy upon rearrangement separately. This calculation may be done following Fuchs,[5] who gave the electrostatic energy per ion as

$$E_{es}=\tfrac{1}{2}Z^{*2}e^2\left\{\frac{4\pi}{\Omega_0}\sum_q{}'\frac{e^{-q^2/4\eta}}{q^2}S^*S-\frac{2\eta^{1/2}}{\pi^{1/2}}+\sum_j{}'\frac{G(\eta^{1/2}r_j)}{r_j}-\frac{\pi}{\eta\Omega_0}\right\}.$$

(We have rewritten his form in our notation.) $G(x)=(2/\sqrt{\pi})\int_{x,\infty}e^{-z^2}dx$. η is a parameter which is selected to obtain good convergence in both sums. We find it most convenient to take the limit as η goes to infinity.

TABLE IV. $\mathcal{V}(r)$ in Ry.

r in a.u.	$\mathcal{V}(r)$
3.6	+0.068
3.74	−0.0100
4.67	−0.0964
5.60	−0.0387
6.54	−0.0126
7.47	+0.0064
8.40	+0.0170
9.34	+0.0089
11.20	−0.0062
13.07	+0.0011

[5] K. Fuchs, Proc. Roy. Soc. (London) **A151**, 585 (1935).

We then find the change in electrostatic energy with a rearrangement at constant volume, and the corresponding change in structure factors $\delta(S^*S)$, as

$$\delta E_{es}=\tfrac{1}{2}Z^{*2}e^2\frac{4\pi}{\Omega_0}\lim_{\eta\to\infty}\sum_q{}'\frac{e^{-q^2/4\eta}}{q^2}\delta(S^*S)\quad\text{per ion.}\quad(3.4)$$

This form is found to converge suitably for the problems we treat, though frequently it is necessary to evaluate certain infinite sums in closed form before taking the limit. This then allows us to treat the problems completely in terms of the change in structure factors.

The computation of the form factors, the energy-wave-number characteristic, and the effective ion-ion interaction given above represents the bulk of the effort in the calculation of a range of electronic and atomic properties. We will now proceed to calculate several such properties.

IV. ELECTRONIC PROPERTIES

1. Fermi Surface

The geometry of the Fermi surface enters directly in a number of topological properties, such as the de Haas-van Alphen effect, magnetoacoustic oscillations, and the anomalous skin effect. It has been recognized[6,7] for some time that a reasonably good account of the Fermi surface of many polyvalent metals could be given in terms of a nearly-free-electron or one-OPW approximation. This is a zero-order approximation in the expansion we

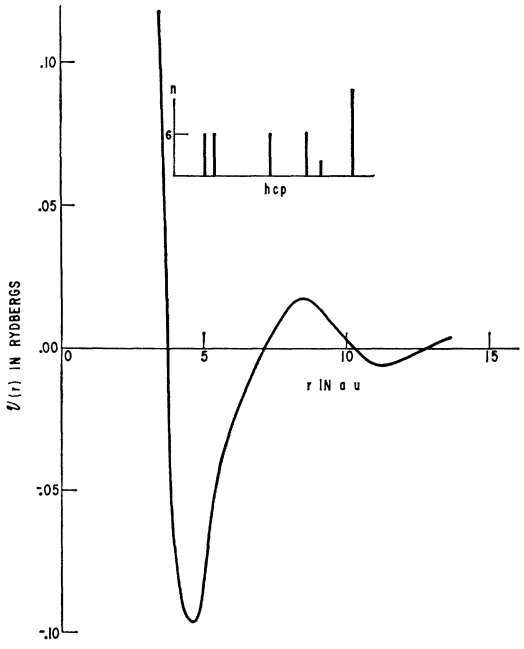

FIG. 4. The effective ion-ion interaction for zinc at the observed density. The number of neighbors, as a function of distance, is shown above for the hcp structure with the observed c/a ratio.

[6] A. V. Gold, Phil. Trans. Roy. Soc. (London) **A251**, 85 (1958).
[7] W. A. Harrison, Phys. Rev. **118**, 1190 (1960).

are using. The agreement can be considerably improved by using OPW form factors as computed above and going to a "few-OPW approximation" as we have done in O. It would appear that the remaining discrepancy arises primarily from errors in the OPW form factors rather than from the limitation in the number of OPW's used, although in cases where the band gaps are quite small the inclusion of more OPW's may invert the ordering of levels. This was found to be the case by L. M. Falicov and G. Weiss (private communication) in magnesium near the point K.

The agreement with the observed Fermi surface which we found in O provides the first check on our calculation.

2. Density of States and dE/dk

The computation of the density of states, which is proportional to the change in volume of a constant energy surface with energy (evaluated at the Fermi surface), is straightforward. For this calculation form factors other than those of Fig. 2 enter. The deviations from the free-electron value are obtained by computing the corrections to the energy at the Fermi surface [the third and final terms of Eq. (3.10) in I which are of the form of the first and second terms in Eq. (3.2) here] and taking the derivative with respect to k. We then average dE/dk over the Fermi surface and compute the density of states. By exact treatment of a two-by-two secular determinant we may show again that taking principal values in the integrals is appropriate. In analogy with the computation of the energy we obtain an equation of the form of Eq. (3.1) with $E(q)$ replaced by a function of wave number representing the change in density of states. This function is to be multiplied by S^*S and summed over wave number space to obtain the density of states.

In zinc the major contribution comes from the twelve lattice wave numbers of the type (1,0,1) for which $q/2k_F=0.952$. The main effect occurs near the intersection of the corresponding zone face and the Fermi surface and we may obtain a good estimate by using a constant form factor corresponding to $\mathbf{q}=-2(0.952)\mathbf{k}$ and $|\mathbf{k}|=k_F$; this value is 0.06 Ry. The correction to the density of states due to these twelve planes corresponds to a thermal mass of $0.91m$. Corrections due to the other lattice wave numbers are very much smaller. Lattice wave numbers for $q<2k_F$ tend to reduce the mass; those for $q>2k_F$ raise it.

The observed[8] density of states mass is $0.93m$. The agreement we find must be regarded as entirely fortuitous. We would expect to find similar theoretical values slightly less than m for other polyvalent metals, but only zinc has an observed mass in this region; aluminum, cadmium, and indium have masses near $1.5m$; mercury and lead are near $2m$. Only gallium ($0.6m$) and zinc have values less than m. We expect to find sizable corrections to the density of states from electron correlations[9] and from the self-energy of electrons due to the electron-phonon interaction.[10] Neither of these corrections have been included in our analysis; they presumably are responsible for the high masses in other metals; but they appear to make little net contribution to the mass in zinc.

Unfortunately, we probably cannot conclude that the observed cyclotron masses in zinc should agree closely with the computed values. An examination of the experimental cyclotron masses of lead by Anderson[11] suggests that the dE/dk corrections are strongly anisotropic. Thus, it may be that some cyclotron masses are raised and some lowered by electron-electron and electron-phonon effects, though the average remains unchanged.

The question arises whether such corrections appear in computations of the resistivity through a modified density of scattered states and through a modified particle velocity. Langer[12] has studied this question in detail with regards to electron-electron interactions. He points out[13] that the problem is more simply viewed in terms of a scattering cross section or mean free path and that these tend not to be affected by electron-electron interactions. Thus, any apparent dependence upon the density of states cancels in the resistivity and our Hartree treatment should be appropriate.

3. Scattering by Defects

We found in I that scattering, to first order in the pseudopotential, could be written as free-electron scattering

$$P_{k+q,k}=(2\pi/\hbar)|\langle\mathbf{k}+\mathbf{q}|W(k)|\mathbf{k}\rangle|^2\delta(T_{k+q}-T_k),$$

where $P_{k+q,k}$ is the probability per unit time of scattering from a state $\mathbf{k}$ to a state $\mathbf{k}+\mathbf{q}$; the matrix elements may be separated into a form factor and a structure factor according to Eq. (2.1). In computing a scattering time for resistivity we multiply the scattering probability by $1-\cos2\Theta$, where 2Θ is again the angle between initial and final states, and sum over final states. The resistivity is then written in terms of this scattering time,

$$\rho=CN\int_0^2|S(q)|^2|\langle\mathbf{k}+\mathbf{q}|w(k)|\mathbf{k}\rangle|^2x^3dx, \qquad (4.1)$$

where $x=q/k$ and $\mathbf{k}+\mathbf{q}$ as well as $\mathbf{k}$ lies on the Fermi surface. N is the number of atoms present and

$$C=3\pi m\Omega_0/8\hbar e^2E_F$$

has the value 1800 $\mu\Omega$ cm per Ry^2 for zinc.

[8] A recent measurement has been made by T. M. Srinivasen, Proc. Indian Acad. Sci. **A49**, 61 (1960).

[9] See, for example, J. G. Fletcher and D. C. Larson, Phys. Rev. **111**, 455 (1958).

[10] J. J. Quinn, in *The Fermi Surface*, edited by W. A. Harrison and M. B. Webb (John Wiley & Sons, Inc., New York, 1960), p. 58.

[11] J. R. Anderson (unpublished).

[12] J. S. Langer, Phys. Rev. **120**, 714 (1960) and **124**, 1003 (1961).

[13] J. S. Langer (private communication).

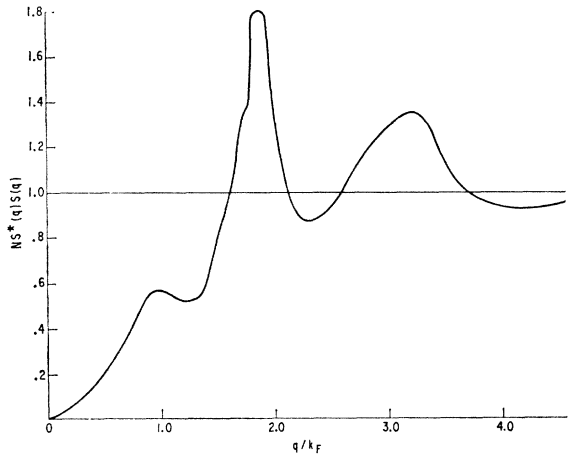

FIG. 5. The square of the structure factor in liquid zinc times the number of atoms present as a function of wave number, obtained from the data of Gamertsfelder (see reference 16).

The form factor appearing in Eq. (4.1) is just that plotted in Fig. 2. We need simply determine $S(\mathbf{q})$ for the defect in question and perform the integral to obtain the resistivity.

The simplest defect is a vacancy (or interstitial) under the assumption that no distortion of the neighborhood occurs. We will examine this assumption when we consider the structure of defects in a later section. For a single undistorted vacancy, a structure factor of magnitude $1/N$ is introduced at every point in wave-number space satisfying periodic boundary conditions in the volume. (We will need to consider these structure factors with more care when we compute the energy of formation of a vacancy.) Thus we obtain the resistivity per vacancy by replacing $S(\mathbf{q})$ by $1/N$ in Eq. (4.1) and integrating. It is convenient and reasonably accurate to approximate the form factor of Fig. 2 by $-0.463+0.269x$. We obtain for the resistivity 0.65 $\mu\Omega$ cm per at.%.

A similar treatment of scattering by vacancy clusters dislocations, stacking faults, or any other defect can be made once one specifies the ion positions. The calculations could be carried to higher order to include the effects of the band structure, but the corrections are small in cases where the first-order scattering is non-vanishing. Freeman[14] has treated the stacking fault in this manner and found that for certain ranges of the angle of incidence no scattering appears in first order, and has carried the analysis to second order.

4. Resistivity of the Liquid

We may proceed with the resistivity of the liquid as we did for static defects. Such an approach is the same as that used by Ziman[15] for the resistivity of the liquid, but the form factors used are more realistic and the somewhat arbitrary separation of structure and plasma terms is unnecessary. We obtain the structure factors from x-ray diffraction experiments, as did Ziman. From the data of Gamertsfelder[16] we determine $N|S(q)|^2$, which we plot against q/k_F (taking k_F for the liquid) in Fig. 5. We use this with the approximate form factor given above and perform the integration (4.1) numerically. We obtain 39 $\mu\Omega$ cm. The experimental value given by Bradley *et al.*[17] is 37 $\mu\Omega$ cm.

The agreement is even closer than we would expect in view of the small discrepancies we found in comparison of the computed form factors and the observed Fermi surface band gaps. It is rather striking that use of the proper form factor has removed all of the discrepancy found by Bradley *et al.*[17] It might also be remarked that in most other respects our treatment of liquids is equivalent to that of Ziman and Bradley *et al.*

5. Electron-Phonon Interaction

Our analysis has contemplated a static arrangement of the ions. However, we may introduce phonons simply by letting the ion positions change with time; our analysis then corresponds to a Born-Oppenheimer approximation. We expand the ion displacements in the form,

$$\delta\mathbf{r}_j=\sum_Q \mathbf{a}_Q(t)\exp(i\mathbf{Q}\cdot\mathbf{r}_j), \tag{4.2}$$

where the $\mathbf{a}_Q$ are regarded as small. Since there are two atoms per cell in zinc we must let $\mathbf{Q}$ run over the double zone in order to allow general displacements. We substitute $\mathbf{r}_j+\delta\mathbf{r}_j$ in the structure factor and expand to second order in $\mathbf{a}_Q$ (only first order is of interest here, but the second order will be needed when we discuss phonon dispersion).

$$S(\mathbf{q})=S^0(\mathbf{q})-\sum_Q i\mathbf{q}\cdot\mathbf{a}_Q S^0(\mathbf{q}-\mathbf{Q}) -\tfrac{1}{2}\sum_{Q,Q'}\mathbf{q}\cdot\mathbf{a}_Q\mathbf{q}\cdot\mathbf{a}_{Q'}S^0(\mathbf{q}-\mathbf{Q}-\mathbf{Q}'), \tag{4.3}$$

where $S^0(\mathbf{q})$ are the structure factors before the introduction of displacement, i.e., delta junctions at the lattice wave numbers, $\mathbf{q}_0$ (2π times the reciprocal lattice vectors).

Thus, a nonvanishing structure factor, with magnitude $-i(\mathbf{q}_0+\mathbf{Q})\cdot\mathbf{a}_Q S^0(\mathbf{q}_0)$ is introduced at each wave vector $\mathbf{q}_0+\mathbf{Q}$ (for every $\mathbf{q}_0$ and every $\mathbf{Q}$).

Let us consider the scattering from a state $\mathbf{k}$ to a state $\mathbf{k}+\mathbf{q}$. Further, let $\mathbf{q}$ lie in the double zone (normal scattering). The corresponding matrix element is given by

$$-i\mathbf{q}\cdot\{S^0(0)\mathbf{a}_q+S^0(-\mathbf{q}_0)\mathbf{a}_{q+q_0}\}\langle\mathbf{k}+\mathbf{q}|w(k)|\mathbf{k}\rangle, \tag{4.4}$$

where $\mathbf{q}_0$ is the one lattice wave number for which $\mathbf{q}+\mathbf{q}_0$ lies in the double zone. The presence of two coefficients, $\mathbf{a}$, corresponds to the fact that there may be scattering by acoustical or optical modes in zinc. We note that the appropriate form factor for these two states is the same

[14] S. Freeman, Jr. (to be published).
[15] J. M. Ziman, Phil. Mag. **6**, 1013 (1961).
[16] C. Gamertsfelder, J. Chem. Phys. **9**, 450 (1941).
[17] C. C. Bradley, T. E. Faber, E. G. Wilson, and J. M. Ziman, Phil. Mag. **7**, 865 (1962).

for acoustical and optical modes, and for longitudinal and transverse polarizations; it is the form factor plotted in Fig. 2. If $\mathbf{q}$ lies outside the double zone (Umklapp) there are two lattice wave numbers for which $\mathbf{q}+\mathbf{q}_0$ lies within the double zone and in the corresponding matrix element both terms appear as the second above with $\mathbf{q}_0$ taking these two values in the two terms.

To determine the scattering by a given phonon, we must determine the structure of the phonon (the relative values of the components of the $\mathbf{a}_Q$'s which enter) and this will be taken up in a later section. For a Debye model of acoustical modes we keep only $\mathbf{a}_Q$'s for $\mathbf{Q}$ in the single hexagonal zone and we obtain immediately three familiar results: pure transverse phonons do not contribute to normal scattering; the matrix element associated with longitudinal scattering are proportional to the corresponding dilatation; the proportionality factor approaches minus two-thirds of the Fermi energy in the long-wavelength limit. It is also interesting to note that in zinc, because the form factor goes through zero, there is no scattering through an angle of about 40°, only larger or smaller angles.

V. ATOMIC PROPERTIES

1. Crystal Structure and c/a Ratio

We choose to compute the band-structure energies of the different crystal structures separately from the electrostatic energy since the latter has been computed and appears in the literature.[18] The difference in electrostatic energy between hexagonal close-packed (ideal c/a), face-centered cubic and body-centered cubic structures is of the order of 10^{-4} Ry per electron and negligible. We wish, however, to compute the variation in the hcp energy with variation of c/a and the contribution of the electrostatic energy there is sizable. We use the computation by Huntington,[19] which in our units is $0.064\,(c/a-1.633)^2$ Ry per electron. The band-structure energy is computed by evaluating the sum $S^*SE(q)$ over lattice wave numbers for the three structures and with varying c/a for hcp. (In all cases the density is taken equal to that observed for zinc.) Contributions for q greater than $3.5k_F$ were obtained by approximating $E(q)$ by $0.15\exp(-2.15q/k_F)$ and the structure factors by a continuum as follows: we note that the sum of S^*S over any sufficiently large volume of wave-number space, $\int d^3q$, is that volume divided by the Brillouin zone volume, Ω_{BZ}. Thus we sum $S^*SE(q)$ over a set of neighboring lattice wave-number points and also evaluate the sum of S^*S for the same set. We then determine a radius, q_s, such that $4\pi q_s^3/3\Omega_{BZ}=1+\sum S^*S$. The one corresponds to the $\mathbf{q}=0$ lattice wave number. The contribution of the more distant lattice wave numbers

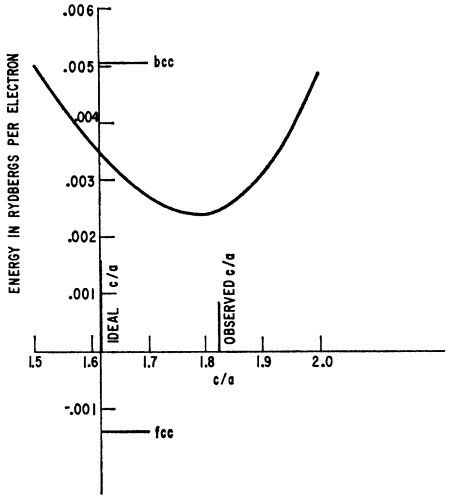

FIG. 6. The computed band-structure energies of hcp, fcc, and bcc zinc (all at a density equal to the observed density). The hcp energy is given as a function of c/a and includes the change in electrostatic energy with departure of c/a from the ideal value. The electrostatic energy for the three structures (with c/a ideal for hcp) is (see reference 18) approximately the same, $-0.312Z^{*2}=-1.271$ Ry per electron.

is then written as

$$\int_{q_s,\infty} d^3qE(q)/\Omega_{BZ}=3\int_{q_s/k_F,\infty} x^2E(k_Fx)dx.$$

We found that if $\sum S^*S$ were taken greater than about 30, the total energy did not depend appreciably upon the choice of $\sum S^*S$ though the magnitude of the continuum contribution was not negligible.

We add to the band-structure energy the electrostatic energy given above to obtain the results shown in Fig. 6. We note first that we find the fcc structure with lower energy than the hcp, contrary to what is observed. We note second that the minimum energy of the hcp structure occurs at approximately the observed ratio. Our failure on the first point represents an error of at least 0.004 Ry per electron, or 0.054 eV per electron. Inspection of $E(q)$ and the structure factors of Fig. 3 makes it clear that variations of this size can be made by reasonable modifications of our interpolations. We conclude that our calculation of $E(q)$ was not sufficiently close-grained to allow a quantitative test of the method. We note, however, that the energy differences obtained are of a reasonable order of magnitude (these energies correspond to temperatures of a few hundreds of deg), and it seems likely that with a slightly more complete calculation, we may be able to compute the most stable structure reliably.

This uncertainty of the interpolation applies also to the determination of the c/a ratio. With a different interpolation we might shift the computed stable c/a ratio significantly. Thus the agreement with the observed ratio must be regarded as fortuitous. Several

[18] W. J. Carr, Jr., Phys. Rev. **122**, 1437 (1961).
[19] H. B. Huntington, in *Solid State Physics*, edited by F. Seitz and D. Turnbull (Academic Press Inc., New York, 1958), Vol. 7, p. 213.

points are worth noting, however. The electrostatic energy rises quadratically with departure from the ideal c/a ratio; it is just the band-structure energy which causes departures. The band-structure energy also reduces the curvature appreciably, a fact which will be discussed in connection with the elastic constants.

Another interesting point may be noted from Fig. 3 where the hcp structure factors are shown, as well as the $E(q)$ curve. The hexagonal face of the double Brillouin zone corresponds to the smallest lattice wave-number ($q=1.63k_F$) and lies in a region for which $dE(q)/dq$ is negative. Thus as the c/a ratio increases and the corresponding q drops, the energy contribution rises. The c/a ratio is higher than ideal *in spite of* the hexagonal face. We find, in fact, that the zone faces which intersect the Fermi surface for all three structures are repelled rather than attracted. This feature of the band-structure energy depends upon the details of the potentials and is not necessarily a general result.

2. Energy Change on Melting

We may compute the band-structure energy of the liquid directly, again using the experimental structure factors of Fig. 5. The sum over wave-number space is replaced by an integral which for a divalent metal may be written in the form,

$$\sum_q S^*SE(q)=3\int NS^*SE(q)(q/k_F)^2d(q/k_F).$$

This integral was performed using the curves of Figs. 3 and 5. The rather surprising result is -0.13 Ry per electron. We see from Fig. 6 that this is significantly lower than the band-structure energy of any of the crystal structures computed. It is not the effects of band structure which favor the formation of a periodic structure, but the electrostatic energy.

We may attempt a computation of the change in electrostatic energy, again using the structure factors from Fig. 5. We use Eq. (3.4) noting that the energy of an ideal gas, for which $S^*S=1/N$ for all q, is zero. We obtain

$$E_{es}=(Z^{*2}e^2k_F/\pi)\int(NS^*S-1)d(q/k_F).$$

This is readily evaluated to obtain -0.65 Ry per electron, some 0.6 Ry per electron higher than that for the crystal structures. This is much too high a value and indicates that the experimental structure factors are not nearly accurate enough to allow a determination of the electrostatic energy. The heat of fusion of zinc is 0.003 Ry per electron. In order to compute the electrostatic energy to sufficient accuracy we would need the area between the curves NS^*S and 1 in Fig. 5 to one part in a thousand; the curve is clearly not that well known.

3. Structure and Energy of Formation of Defects

It seems easier, at least conceptually, to compute the structure of defects using $\mathcal{U}(r)$ rather than $E(q)$. The $\mathcal{U}(r)$ curve which we have computed would seem not sufficiently well determined to warrant a detailed treatment of the structure of any defect. However, we may note some interesting features by considering a vacancy. It can be seen from Fig. 4 that $d\mathcal{U}(r)/dr$ is positive and rather large for the twelve nearest neighbors. Thus, if we remove a single atom from the lattice, the unbalanced force on the nearest neighbors is outward, and they suffer a first-order outward displacement. The first-order displacement of the next-nearest neighbors is also outward, but smaller. These displacements bring the nearest and next-nearest neighbors closer together and increase the attraction between them; thus the second-order displacements also tend to bring these closer together. Without carrying out the detailed minimization of the energy we obtain a picture of the vacancy structure: the vacancy is slightly larger than it would be without displacements, but the ion density immediately surrounding the vacancy is higher than normal. It is not clear what the long-range displacements are. We should also remark that this conclusion is rather sensitive to the position of the sharp minimum in Fig. 4 and is, therefore, open to question.

We may also estimate the energy of formation of a vacancy. We do this for an undeformed vacancy and thus tend to overestimate the energy slightly. We must take care in the energy calculation to keep the total number of ions fixed and to keep the volume fixed. Thus, we compare the energy of N ions in the perfect lattice corresponding to the lattice wave numbers $\mathbf{q}_0$ with N ions in a lattice with wave numbers $\mathbf{q}_0'$ and a vacancy. The $\mathbf{q}_0'$ are increased according to $\mathbf{q}_0'=[1+1/(3N)]\mathbf{q}_0$ in order to keep the volume fixed. The structure factors in the lattice with a vacancy associated with $\mathbf{q}_0'$ are equal to those in the perfect crystal for the corresponding $\mathbf{q}_0$. In addition, structure factors with magnitude $1/N$ are introduced at every other $\mathbf{q}$ satisfying periodic boundary conditions in the volume.

We first compute the difference in band-structure energy. The contribution to the total band-structure energy [note that $E(q)$ gives the energy per electron] from the continuum of structure factors $1/N$ is found to be $3Z\int E(q)x^2dx$, with $x=q/k_F$. This we may evaluate from our $E(q)$ curve to obtain -1.52 Ry. The change in band-structure energy due to the shift of the lattice wave numbers is $(Z/3)\sum_{q_0}S^*Sq_0\partial E(q_0)/\partial q_0$. This is found to be about -0.04 Ry. The change in electrostatic energy is computed in a similar way using Eq. (3.4). We obtain $-(2/3)$ the electrostatic cohesive energy per ion. With our effective charge this leads to 1.69 Ry. The total energy of formation, then, is found to be 0.13 Ry or 1.8 eV.

This would appear to be an overestimate; the activa-

tion energy for self-diffusion, which includes the energy of formation and the energy of motion, is about one electron volt.[20] However, we are in this case computing the difference between large quantities (the band-structure energy and the electrostatic energy differ by less than a tenth of either) so the error in the band-structure energy is less than 10%, which is gratifying. We further note that the main contribution to the change in band-structure energy comes from the region of small q, so a little more care in this region may easily improve the agreement.

4. Elastic Constants

There are three independent, volume-conserving shear strains in hexagonal metals.[19] One of these corresponds to a change in the c/a ratio at constant volume and the corresponding elastic constant can be obtained directly from Fig. 6. We fit the energy values at $c/a=1.5$, 1.8, and 2.0 with a parabola and obtain the elastic constant from the quadratic term. We obtain $c_{11}+c_{12}+2c_{33}-4c_{13}=30\times10^{11}$ dyn/cm^2. The experimental value given by Huntington[19] is 11.7. We note that the value from the electrostatic energy alone is 45, so our error in the band structure contribution is a factor of two. This discrepancy is not at all surprising in view of the uncertainty in the parabolic approximation to our interpolated curves. We may also note that the neglect of core-core interactions is much more serious in computing elastic constants than in computing energies. It is interesting to note that the effect of band structure is to reduce the elastic constants significantly.

An attempt was made to compute the band structure contributions to the other two shear constants. They were found to be small, as they should be; the numbers obtained were within error of zero.

5. Stabilization of Structures

We wish to make two comments concerning the ordering of alloys though these are not strictly within the domain of our analysis. It would probably be most convenient to formulate the theory of a binary alloy in terms of a form factor which is the average of that for the two components and one which, for each component, is the difference from the average. We can then focus our attention on the term from the difference. We may find that, just as in the study of the liquid, the band-structure energy is lower in the disordered alloy; if then Z^* is the same for both components, the alloy will not order at any temperature.

Sato and Toth[21] have met with significant success in correlating the ordering distance in binary alloys with Brillouin zone faces tangent to the surface, so-called stabilization. Clearly on any simple model, the energy due to a zone face drops monotonically as that face is brought in through the Fermi surface. Thus stabilization does not exist in three dimensions unless the effective band gap has an accidental maximum in this region. We see from Fig. 3 that there does exist a sharp minimum in $E(q)$ in zinc which arises from the maximum form factors seen in Fig. 1. If we are to explain the stabilization in terms of a similar effect in the systems studied by Sato *et al.*, we must assume that this minimum moves with the Fermi surface during alloying. Clearly our calculation on a single metal does not tell us whether such a movement is to be expected.

It is interesting to note that the prominent minimum in $E(q)$ derives almost entirely from the orthogonalization corrections [first term in Eq. (3.2)] which would be entirely absent in a wave-number-independent pseudopotential approximation.

6. Phonon Structure and Dispersion

We proceed with the construction of the phonon as in Sec. IV 5. We include two amplitude vectors, $\mathbf{a}_Q$ and $\mathbf{a}_{Q'}$, corresponding to wave numbers in the double zone and differing by $2\pi/c$ in their component along the c axis. We also include $\mathbf{a}_{-Q}=\mathbf{a}_Q{}^*$ and $\mathbf{a}_{-Q'}=\mathbf{a}_{Q'}{}^*$. The structure factors are given by Eq. (4.3). We find second-order corrections to S^*S at lattice wave numbers, $\mathbf{q}_0$, which had nonzero structure factors in the perfect lattice, and values of S^*S which are second order in the $\mathbf{a}$'s at wave numbers, $\mathbf{q}_0\pm\mathbf{Q}$. Each of these second-order terms, in general, depends both on $\mathbf{a}_Q$ and $\mathbf{a}_{Q'}$. The change in energy may be written in terms of these structure factors and is a quadratic form in the six components of the $\mathbf{a}$'s. The coefficients depend upon $E(q)$. We may also write the kinetic energy as a quadratic form in the $\dot{\mathbf{a}}$'s. This results in the problem of computing the normal modes (the structure of the corresponding phonons) and vibration frequencies of a system with six degrees of freedom.

We restrict our attention here to the interesting case in which $\mathbf{Q}$ is parallel to the c axis and very near zero; $\mathbf{Q}'$ is parallel to the c axis and very near $-2\pi/c$. We first let $\mathbf{Q}$ approach zero and keep only terms which are zero-order in $\mathbf{Q}$. We compute a correction to S^*S near each $\mathbf{q}_0$ by adding the modified S^*S at $\mathbf{q}_0$ to those at $\mathbf{q}_0\pm\mathbf{Q}$ and subtracting the initial S^*S. We find that only the $\mathbf{a}$ and $\mathbf{a}^*$ corresponding to $\mathbf{Q}'$ enter; these modes will correspond to the optical modes. We find corrections to the structure factors given by $S^*S=(-1)^{n+1}2|\mathbf{q}_0\cdot\mathbf{a}_{Q'}|^2$ for $q_0=2\pi n/c$ and parallel to the c axis, and $S^*S=(-1)^n|\mathbf{q}_0\cdot\mathbf{a}_{Q'}|^2$ for q_0 having a lateral component equal to the smallest lattice wave number in the basal plane ($4\pi/3^{1/2}a$) and component along the c axis equal to $2\pi n/c$. Contributions of the more distant $\mathbf{q}_0$ to the energy are negligible. There are no cross terms between components of $\mathbf{a}_{Q'}$ parallel and perpendicular to the c axis, so we obtain pure longitudinal and pure transverse waves; the transverse waves are degenerate. We

[20] G. A. Shirn, E. S. Wajda, and H. B. Huntington, Acta Met. 1, 513 (1953).
[21] H. Sato and R. S. Toth, Phys. Rev. 127, 469 (1962).

compute the band-structure energy associated with the first set ($\mathbf{q}_0$ parallel to the c axis) by summing through $n=3$, and with the second set by summing through $n=2$. We obtain for the longitudinal wave ($|\mathbf{a}_{Q'}|=a'$ parallel to c axis) a band-structure energy of $-0.93a'^2$ Ry/ion if a' is in atomic units. For the transverse wave we obtain $-0.035a'^2$ Ry/ion if a' is in atomic units (a.u.). Similarly we may compute the electrostatic energy for these two cases from Eq. (3.4). For the longitudinal wave we find the electrostatic energy, within about 1%, by summing only along the c axis from $-\infty$ to ∞ before letting η go to infinity. We obtain $4\pi Z^{*2}e^2a'^2/\Omega_0$ per ion, or $0.99a'^2$ Ry/ion. For the transverse wave almost the entire electrostatic energy is obtained by summing over the six lines parallel to the c axis and through the smallest transverse lattice wave numbers. We obtain for the electrostatic energy $(12\pi Z^{*2}e^2\xi a'^2/\Omega_0)/(e^{\xi}-e^{-\xi})$, per ion with $\xi=(2\pi 3^{-1/2})\times(c/a)$. This corresponds to $0.026a'^2$ Ry/ion.

We find that the band-structure contribution and the electrostatic contribution tend to cancel in both cases. We find in fact that the band-structure term dominates in the case of the transverse wave and thus that the crystal is unstable against the corresponding distortion. This incorrect result is related to our earlier finding that the fcc structure was lower in energy than the hcp structure. The fcc stacking of close-packed planes is found to have lower energy than the hcp stacking; similarly, the change in stacking corresponding to an optical transverse wave propagating parallel to the c axis also is found to have lower energy. We may compute a frequency for the longitudinal optical mode from the above numbers; we obtain 3.3×10^{12} cps. This is in remarkable agreement with the value of 3.5×10^{12} cps found experimentally by Joynson.[22] It may also be contrasted with the value obtained from the electrostatic energy alone, 13.2×10^{12} cps.

We could proceed in the same way for the acoustical waves, keeping terms to second-order in $\mathbf{Q}$. In the long-wavelength limit we expect only the $\mathbf{a}$'s corresponding to $\mathbf{Q}$ to enter, and the longitudinal and transverse waves to separate. The computation proceeds as with the optical modes, but the first and second derivatives of $E(q)$ enter, as well as $E(q)$ itself. For the long-wavelength limit, it is probably simplest to treat the transverse waves in terms of shear constants computed as in the preceding subsection.

The longitudinal acoustic waves cannot be treated in terms of a uniform distortion without violating our condition of rearrangement at constant volume so we consider the waves. On physical grounds we know that this must yield the same answer as if we had retained the diagonal terms in the Hamiltonian and computed the differential change in energy under a uniform expansion. Rather than estimate the second derivatives of $E(q)$ which enter as $\mathbf{Q}$ goes to zero, we chose to compute the frequency at the center of the hexagonal face of the single zone. At this point the acoustical and optical modes are degenerate. We consider longitudinal polarization vectors $\mathbf{a}_{\pi/c}$ and $\mathbf{a}_{-\pi/c}=\mathbf{a}_{\pi/c}^*$. A particular mode is selected by taking the $\mathbf{a}$'s to be real and the energies found to second order in the $\mathbf{a}$'s and $\dot{\mathbf{a}}$'s as above. The electrostatic energy is found to be formally identical to that for the longitudinal optical mode given above while the mass factor in the kinetic energy is doubled; thus we find the frequency based only on the electrostatic energy lower by $\sqrt{2}$. On the other hand, the magnitude of the band-structure term is increased by more than 30%, it dominates the electrostatic term, and we find an instability as we did for the optical transverse mode.

7. Kohn Effect

The Kohn effect[23] is, in principle, included in this treatment. We use Hartree screening, which gives rise to a singularity in $E(q)$ at $q=2k_F$. This singularity is not visible in Fig. 3 and it is in fact very slight. Woll and Kohn[24] have shown that the resultant singularities in the phonon dispersion should only be observable under very favorable circumstances. It has, therefore, been surprising that irregularities do show up in dispersion curves,[25] though not quite at the wave numbers expected.

A likely resolution of this puzzle may be seen in Fig. 3. Any irregularity in $E(q)$ will cause corresponding irregularities in the phonon dispersion curve. The sharp oscillation seen there should cause a sharp oscillation in the dispersion curve. This need not occur at precisely $2k_F$ though it may, as in zinc, be in roughly this position. We therefore suggest that the irregularties observed by Brockhouse *et al.*[25] are not images of the Fermi surface, but images of the energy-wave-number characteristic.

8. Experimental Determination of the Energy-Wave Number Characteristic

The fact that $E(q)$ enters so directly in phonon dispersion and that the spectrum spans a large segment of wave-number space suggests it as a tool for the experimental determination of $E(q)$. It is appropriate first to compute the electrostatic contribution to the energy associated with a given phonon and subtract it from the energy obtained from the experimental frequency. One then deduces the band-structure contribution from which the $E(q)$ curve is to be obtained.

It is clear that $E(q)$ cannot be uniquely determined in this way. This is most easily seen by considering the dependence upon $U(r)$, which is the Fourier transform of $E(q)$. The phonon spectrum is completely determined

[22] R. E. Joynson, Phys. Rev. **94**, 851 (1954).

[23] W. Kohn, Phys. Rev. Letters **2**, 393 (1959).

[24] E. J. Woll, Jr., and W. Kohn, Phys. Rev. **126**, 1693 (1962).

[25] B. N. Brockhouse, K. R. Rao, and A. D. B. Woods, Phys. Rev. Letters **7**, 93 (1961); B. N. Brockhouse, T. Arase, G. Caglioti, K. R. Rao, and A. D. B. Woods, Phys. Rev. **128**, 1099 (1962).

by the first and second derivatives of $\mathcal{U}(r)$ at the *observed* interatomic distances. Thus $\mathcal{U}(r)$ is not uniquely determined by the spectrum, nor is its transform. It is therefore necessary to postulate a form for $E(q)$ and fit parameters.

This attempt has been made for lead using the accurately determined dispersion curves of Brockhouse *et al.*[25] We found that the results were sufficiently sensitive to the form of the postulated $E(q)$ curve that no meaningful curve could be obtained. We conclude that a rather reliable $E(q)$ must be obtained first theoretically, which could then be improved by adjusting to fit the observed spectrum. Because of the uncertainty of the effect of core-core interactions in zinc it did not seem appropriate to carry out this rather extensive analysis for zinc.

VI. CONCLUSIONS

Though we have not been entirely successful in the quantitative computation of properties, much can be learned from the analysis.

We find that the rather rough calculation which one is able to do on a desk machine seems to suffice for the determination of the OPW form factors. The single curve, corresponding to initial and final states on the Fermi surface, enables the quantitative computation of a sizable array of electronic properties. We found that our results were quite accurate for the determination of the Fermi surface and the resistivity of the liquid. We also found agreement with the observed electronic specific heat but did not expect such agreement would be found in other polyvalent metals. Electron-electron and electron-phonon effects enter the density of states directly but seem not to affect the result in zinc. These effects are not expected to enter the resistivity nor the Fermi surface in any case.

In considering other polyvalent metals we may note that in all cases the form factor approaches $-\frac{2}{3}E_F$ as q goes to zero. Further, in any polyvalent metal which is rather free-electron-like, the form factors must be near zero at q near $2k_F$. Thus, we may expect the form-factor curve to be very much the same for other polyvalent metals as it is for zinc.[25a]

We find that the OPW form factor curve in question is a rather straight line in zinc. This suggests a phenomenological approach in cases where one does not wish to carry out the complete calculation. One knows the $q=0$ intercept and needs only one other point on the curve. This may be obtained from an existing band calculation or even from an experimentally known Fermi surface. In the latter case there is the ambiguity of sign discussed in O, but if more than one gap is known the signs can be determined readily if the form factor is in fact roughly a straight line.

We found that the calculation of the energy-wave-number characteristic would have to be improved significantly for a quantitative test of the method for computing atomic properties. It was apparent in particular that the $E(q)$ would need to be computed for more values of q. Further, it may be necessary to compute more OPW form factors to avoid the interpolation we required for the summation over states. Finally, in zinc it may be essential to include the effects of core-core interaction, particularly in the treatment of the change in energy upon melting and the elastic properties. While we obtain semiquantitative agreement with some properties, in others we obtain errors in sign for the difference between band structure and electrostatic energy and resulting instabilities against rearrangement.

On the whole, we regard the results as encouraging. The computed band-structure energy entering the atomic properties appeared in all cases to be semiquantitatively correct. This implies that the band structure effects are as small as we find and therefore that the perturbation approximation is justified. The validity of neglecting changes in core states would be much greater in other metals. Thus, assuming only that the Hartree approximation is sufficiently accurate, the method should be capable of giving reliable results. A more careful computation of $E(q)$, using high-speed computers, is much to be desired. Magnesium, aluminum, or gallium would seem to be likely choices; also possibly sodium.

It would also be of interest to use the method phenomenologically; that is, to adjust a computed $E(q)$ to fit the observed phonon spectrum and to use this experimental characteristic to compute a range of properties.

It seems at first surprising that large band-structure effects are present when the Fermi surface is so free-electron-like. It will be recalled that when Leigh[26] fit a band structure for aluminum to the observed elastic constants, he found very large deviations from a free-electron Fermi surface. The primary feature of our calculation which explains this result is the very steep slope of the $E(q)$ curve, corresponding to matrix elements which change very rapidly with wave number. Thus, when the lattice is distorted and the zone faces displaced, the band gaps change very rapidly. Thus the important terms are the change in band structure under distortion rather than the redistribution of electrons in a rigid band structure.

Another feature of our calculation, which is not apparent from the results alone, is the relative contribution of various terms. It turns out that $E(q)$ in the important region near $q=2k_F$ is determined almost entirely by the first term in Eq. (3.2). This term arises from the non-orthogonality of OPW's or equivalently from

[25a] *Note added in proof*. We have recently made calculations of the OPW form factors corresponding to initial and final states at the Fermi surface for all nontransition metals with atomic number less than that of zinc (results to be published). The resulting curves for each of the polyvalent metals (Be, Mg, Al, and Ca) are strikingly close to that for zinc if all curves are plotted in units of the Fermi energy for the metal in question.

[26] R. S. Leigh, Phil. Mag. **42**, 139 (1951).

the nonhermiticity of the pseudopotential. The inclusion of this term does not introduce any band gaps at the zone faces, but simply deforms the bands slightly. Thus we obtain the main qualitative features of the atomic properties before we introduce the familiar band-structure effects at the zone faces. It is also interesting to note that this term is absent in a wave-number-independent pseudopotential approximation.

We have found the computation of the atomic properties in terms of a sum over wave number of the energy-wave-number characteristic more convenient for almost all properties we consider than the equivalent sum over neighbors of the effective ion-ion interaction, $\mathcal{U}(r)$. When the electrostatic energy is computed separately the convergence of the band-structure energy is quite rapid. It may be seen from Fig. 4 that the forces (the derivative of Fig. 4) are very appreciable well beyond six sets of neighbors (38 neighboring atoms) so that the convergence using $\mathcal{U}(r)$ is certainly no more rapid. Furthermore, the computation of $\mathcal{U}(r)$ requires taking the Fourier transform of $E(q)$ which may introduce further error. It has been rather striking that such a wide range of properties can be computed so simply once the energy-wave-number characteristic is known.

It should be noted that we have included in the band-structure energy all of the screening. One might suggest that this is the only important contribution to the band-structure energy and thus that one could hope to compute most of these properties simply using Hartree screening of the net Coulomb potential of the ion without concern for the detailed structure of the ion. We may show that this is not the case.

The electronic properties depend on the OPW form factor curve given in Fig. 2. To be sure, with simple screening, we obtain the correct value, $-\frac{2}{3}E_F$, in the long-wavelength limit, and the curve rises as q approaches $2k_F$. However, it rises only to about -0.15 Ry; thus we lose completely the free-electron-like behavior which characterizes the metal so well.

The atomic properties are described in terms of the energy-wave-number characteristic. If we compute this characteristic with Hartree screening of point ions, we again obtain results which are roughly correct in the long-wavelength limit. This is reflected in the success of the Bohm-Staver[4] treatment of the speed of long-wavelength longitudinal acoustical modes. However, every other property we have considered depends most strongly on the characteristic in the region $q \approx 2k_F$, and the structure of the curve in this region derives entirely from the details of the ion potential.

To be quantitative, it is a simple exercise to carry out the analysis we have used for a simple potential (no wave-number dependence). If that simple potential is the Coulomb potential for point ions of charge Ze, we obtain $E(q)=(4\pi e^2Z/\Omega_0 q^2)(1-\epsilon_q)/2\epsilon_q$. We may add the electrostatic and band-structure energy and find it to be given by the electrostatic energy of Eq. (3.4) with each term divided by the Hartree dielectric function ϵ_q. [This means that the effective ion-ion interaction $\mathcal{U}(r)$ for this case is simply the screened Coulomb interaction, a result included in Cohen's[27] Eq. (7).] We have carried out this analysis for lead and computed the velocity of sound in the [110] direction. For the longitudinal wave we obtain 3.88 (in units of 10^5 cm/sec) compared to the Bohm-Staver value (uniform positive background rather than point ions) of 3.44. Thus the discrepancy with the observed[25] 2.43 is increased. For the transverse wave with polarization parallel to the $[1\bar{1}0]$ direction we found 2.75 which is higher than the value 1.07 based upon the electrostatic energy alone and than the observed[25] 0.64. For the transverse wave with polarization parallel to [001] we obtain 2.88 to be compared with the electrostatic value of 3.21 and the experimental[25] 1.26. These large corrections occur because the derivatives of $E(q)$ and, therefore, of the dielectric function enter. Clearly the inclusion of screening does not eliminate the large discrepancies of the electrostatic approximation.

If one concludes thus that the major correction comes from the structure of the ion, one might still suggest a simple treatment in terms of a wave number independent pseudopotential approximation. We found that the wave number dependence was very strong and important, as indicated in Fig. 1, so such an approach is certainly not useful for a calculation from first principles. However, one might wish to use it phenomenologically. To be sure, one may define from the OPW form factor of Fig. 2 an equivalent effective potential, and from the energy wave number characteristic an equivalent effective potential but these form significantly different potentials so we gain nothing at all; it is simply replacing one unknown curve by another. That these two potentials are not the same can be seen most strikingly by noting again that the term in the $E(q)$ computation which most strongly influences the character of $E(q)$ is not the second term in Eq. (3.2), which resembles ordinary second-order perturbation theory, but the first term which derives from the nonorthogonality of OPW's.

We find that the simplifications of the theory which we have considered do not contain the important features of the problem. We might also ask if we can readily improve our calculation by carrying it to higher order. We note that if we carry the screening to higher order, the potential to be associated with each ion then depends upon the arrangement of the ions. Thus, the separation into structure-dependent and potential-dependent terms is no longer possible; the OPW form factor and the $E(q)$ term lose their meaining. In terms of the effective ion-ion interaction, this means that we pass from two-body to multibody interactions, as indicated by Cohen.[27] We conclude that the most straightforward improvement of the calculation makes the computations immensely more complex.

---

[27] M. H. Cohen, paper contributed to Colloquium on The Structure of Metallic Solid Solutions, Orsay, France), July 9–11, 1962 (to be published in the Proceedings of the Colloquium).